J. Fluid Mech. (2024), *vol*. 992, A9, doi:10.1017/jfm.2024.545

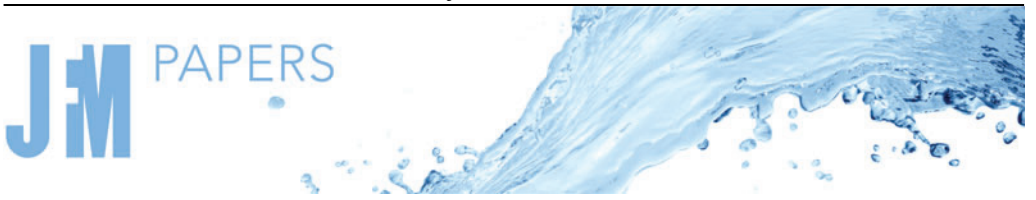

Non-universality and dissipative anomaly in compressible magnetohydrodynamic turbulence

Cheng Li[1,2], **Yan Yang**[3], **William H. Matthaeus**[3], **Bin Jiang**[1,2], **Minping Wan**[1,2,†] **and Shiyi Chen**[4,1,2]

[1]Guangdong Provincial Key Laboratory of Turbulence Research and Applications, Department of Mechanics and Aerospace Engineering, Southern University of Science and Technology, Shenzhen 518055, PR China

[2]Guangdong-Hong Kong-Macao Joint Laboratory for Data-Driven Fluid Mechanics and Engineering Applications, Southern University of Science and Technology, Shenzhen 518055, PR China

[3]Department of Physics and Astronomy, University of Delaware, DE 19716, USA

[4]Eastern Institute for Advanced Study, Eastern Institute of Technology, Ningbo 315200, PR China

(Received 8 February 2024; revised 2 May 2024; accepted 28 May 2024)

We systematically study the dissipative anomaly in compressible magnetohydrodynamic (MHD) turbulence using direct numerical simulations, and show that the total dissipation remains finite as viscosity diminishes. The dimensionless dissipation rate $\mathcal{C}_\varepsilon$ fits well with the model $\mathcal{C}_\varepsilon = \mathcal{C}_{\varepsilon,\infty} + \mathcal{D}/R_L^-$ for all levels of flow compressibility considered here, where R_L^- is the generalized large-scale Reynolds number. The asymptotic value $\mathcal{C}_{\varepsilon,\infty}$ describes the total energy transfer flux, and decreases with increase of the flow compressibility, indicating non-universality of the dimensionless dissipation rate in compressible MHD turbulence. After introducing an empirically modified dissipation rate, the data from compressible cases collapse to a form similar to the incompressible MHD case depending only on the modified Reynolds number.

Key words: turbulence theory, MHD turbulence, compressible turbulence

1. Introduction

Dissipative anomaly states that ε, the rate of turbulent energy dissipation (per unit mass) away from boundaries, remains finite as viscosity tends to zero (Taylor 1935). As a basic hypothesis of the K41 turbulence theory (Kolmogorov 1941*a*,*b*,*c*; Frisch 1995), it is of fundamental importance and is often deemed as the 'zeroth law of turbulence'. Understanding dissipative anomaly was primarily phenomenological until the pioneering theoretical study of Onsager (1949). His work established a crucial connection between

† Email address for correspondence: wanmp@sustech.edu.cn

finite dissipation in hydrodynamic (HD) turbulence and the inherent roughness of velocity field. Onsager's conjecture was then proved rigorously under different assumptions (Constantin, Weinan & Titi 1994; Eyink 1994; Duchon & Robert 2000), and extended to diverse turbulence systems as well, including incompressible magnetohydrodynamic (IMHD) turbulence (Aluie 2017), incompressible Hall magnetohydrodynamic (MHD) turbulence (Galtier 2018), and compressible HD turbulence (Eyink & Drivas 2018).

Dissipative anomaly has been well explored by experiments and simulations in HD turbulence (Sreenivasan 1984, 1998; Kaneda *et al.* 2003; Pearson *et al.* 2004; Mazellier & Vassilicos 2008; Goto & Vassilicos 2009; McComb *et al.* 2015; Vassilicos 2015; John, Donzis & Sreenivasan 2021) and IMHD turbulence (Mininni & Pouquet 2009; Dallas & Alexakis 2014; Linkmann *et al.* 2015; Linkmann, Berera & Goldstraw 2017; Bandyopadhyay *et al.* 2018). In practice, the interest centres on the dimensionless dissipation rate

$$\mathcal{C}_\varepsilon = \varepsilon \mathcal{L}/\mathcal{U}^3 \tag{1.1}$$

and its asymptotic value $\mathcal{C}_{\varepsilon,\infty}$ as Reynolds number tends to infinity, where $\mathcal{U}$, $\mathcal{L}$ denote the characteristic values of velocity and length, respectively. Non-universality of $\mathcal{C}_{\varepsilon,\infty}$ was investigated in various turbulent flows, with varying vector field correlations (Linkmann *et al.* 2015, 2017) and anisotropy (Bandyopadhyay *et al.* 2018).

In turbulent flows with more intricate configurations, the energy dissipation properties can be notably influenced by a variety of phenomena and structures. For instance, in oceanic or stratified geophysical flows, interactions between eddies, waves, drafts and fronts in these environments contribute to the complexity of energy dissipation dynamics (Pearson & Fox-Kemper 2018; Pouquet, Rosenberg & Marino 2019; Marino *et al.* 2022). Similarly, in compressible MHD turbulence, the interplay between vortices, shocks and Alfvén waves adds additional complexity, leading to a significantly expanded parameter space. As a result, the understanding of dissipative anomaly in compressible MHD turbulence remains limited.

In this paper, we study the dissipative anomaly in compressible MHD turbulence by performing direct numerical simulations of forced compressible MHD turbulence, without background magnetic field and cross-helicity. The compressibility effect on the dissipative anomaly is explored quantitatively. We propose a unified model that explains the normalized dissipation rate and its variation with compressibility.

2. Equations and numerical simulations

By introducing the reference scales ρ_0 for density, U_0 for velocity, B_0 for magnetic induction, L_0 for length, T_0 for temperature, $\rho_0 U_0^2$ for pressure, μ_0 for dynamic viscosity, η_0 for magnetic diffusivity, and κ_0 for thermal conductivity, the compressible MHD system involves five dimensionless parameters: the Reynolds number $Re = \rho_0 U_0 L_0/\mu_0$, the magnetic Reynolds number $Re_m = U_0 L_0/\eta_0$, the Mach number $M = U_0/\sqrt{\gamma R T_0}$, the Alfvén Mach number $M_m = U_0\sqrt{\rho_0}/B_0$, and the Prandtl number $Pr = \mu_0 C_p/\kappa_0$, where $\gamma = 1.4$ denotes the adiabatic index, R the gas constant, and $C_p = \gamma R/(\gamma - 1)$ the specific heat at constant pressure. The dimensionless governing equations are

$$\partial_t \rho + \boldsymbol{\nabla} \cdot (\rho \boldsymbol{u}) = 0, \tag{2.1}$$

$$\partial_t (\rho \boldsymbol{u}) + \boldsymbol{\nabla} \cdot \left(\rho \boldsymbol{u}\boldsymbol{u} + p_t \boldsymbol{I} - \frac{\boldsymbol{b}\boldsymbol{b}}{M_m^2} \right) = \frac{\boldsymbol{\nabla} \cdot \boldsymbol{\sigma}}{Re} + \mathcal{F}, \tag{2.2}$$

$$\partial_t \boldsymbol{b} + \boldsymbol{\nabla} \cdot (\boldsymbol{u}\boldsymbol{b} - \boldsymbol{b}\boldsymbol{u}) = -\frac{\boldsymbol{\nabla} \times (\eta \boldsymbol{j})}{Re_m}, \tag{2.3}$$

$$\partial_t E + \boldsymbol{\nabla} \cdot \left[(E + p_t)\boldsymbol{u} - \frac{(\boldsymbol{u} \cdot \boldsymbol{b})\boldsymbol{b}}{M_m^2} \right] = \frac{\boldsymbol{\nabla} \cdot (\boldsymbol{\sigma} \cdot \boldsymbol{u})}{Re} + \frac{\boldsymbol{\nabla} \cdot (\boldsymbol{b} \times \eta \boldsymbol{j})}{Re_m M_m^2} + \frac{\boldsymbol{\nabla} \cdot (\kappa \boldsymbol{\nabla} T)}{Pr\, Re\, (\gamma - 1) M^2} + \mathcal{F} \cdot \boldsymbol{u} - \Lambda, \tag{2.4}$$

where ρ, $\boldsymbol{u}$, $\boldsymbol{b}$ and T are the density, velocity, magnetic and temperature fields, respectively. Here, $E = \rho \boldsymbol{u}^2/2 + p/(\gamma - 1) + \boldsymbol{b}^2/(2M_m^2)$ denotes the total energy, $p_t = p + \boldsymbol{b}^2/(2M_m^2)$ the total pressure, $\boldsymbol{\sigma} = 2\mu(\boldsymbol{S} - \theta \boldsymbol{I}/3)$ the viscous stress tensor, $\boldsymbol{S} = (\boldsymbol{\nabla u} + \boldsymbol{\nabla u}^{\mathrm{T}})/2$ the strain rate tensor, $\theta = \boldsymbol{\nabla} \cdot \boldsymbol{u}$ the dilatation, $\boldsymbol{I}$ the unit tensor, and $\boldsymbol{j} = \boldsymbol{\nabla} \times \boldsymbol{b}$ the current density. Closure is achieved using the ideal gas law $p = \rho T/(\gamma M^2)$. For simplicity, we set $Pr = 0.704$, $Pr_m = Re_m/Re = 1$ and $M_m = 1$. The dimensionless constitutive coefficients μ, κ, η obey Sutherland's law of air with reference temperature $T_0 = 273.15\,\mathrm{K}$, $\mu = \kappa = 1.40417T^{3/2}/(T + 0.40417)$ and $\eta = \nu = \mu/\rho$, where ν is the kinematic viscosity. To attain a statistically steady state, a large-scale force $\mathcal{F}$ and cooling function Λ are imposed in the momentum and energy equations, respectively.

Direct numerical simulations (DNS) of compressible MHD turbulence are performed in a periodic $(2\pi)^3$ cubic domain, using a hybrid compact-WENO scheme (Wang *et al.* 2010; Yang *et al.* 2016*b*). This hybrid scheme, known for its high accuracy and efficiency in handling shock–turbulence interaction in compressible turbulent flows, generates negligible numerical dissipation (Yang *et al.* 2021), thus guarantees the reliability of the numerical results presented in this study. To control the compressibility, the large-scale force $\mathcal{F}$ modifies the compressive (dilatational) velocity field $\boldsymbol{u}_c$ and solenoidal velocity field $\boldsymbol{u}_s$ in the first two wavenumber shells. These are defined by the Helmholtz decomposition (Wang *et al.* 2012; Yang *et al.* 2016*b*, 2017)

$$\boldsymbol{u} = \boldsymbol{u}_s + \boldsymbol{u}_c, \quad \boldsymbol{\nabla} \cdot \boldsymbol{u}_s = 0, \quad \boldsymbol{\nabla} \times \boldsymbol{u}_c = 0. \tag{2.5a–c}$$

The parameter r_c regulates the fraction of the energy input into the compressive field $\boldsymbol{u}_c$. The limiting conditions $r_c = 1$ and 0 represent pure dilatational and pure solenoidal forcing, respectively. For more simulation details, see Yang *et al.* (2016*b*).

A number of simulations with resolution up to 768^3 were performed, and grouped into eight different series, based on Mach number M and forcing parameter r_c. All statistical quantities are obtained by averaging (denoted by $\langle\,\rangle$) over 80 snapshots spanning at least 6 large-eddy turnover times, after the flow reaches the statistically steady state. Basic simulation parameters are the Taylor microscale Reynolds number $R_\lambda = 23$–386, the turbulent Mach number $M_t = 0.2$–0.69, and $\delta_c = u_c'/u' = 0.36$–$0.94$. The parameter δ_c represents the relative magnitude of the compressive velocity and the flow compressibility, where $u' = \sqrt{\langle \boldsymbol{u}^2 \rangle/3}$ and u_c' denote the root mean square (r.m.s.) values of the components of the vectors $\boldsymbol{u}$ and $\boldsymbol{u}_c$, respectively. All simulations are fully resolved such that $k_{max}\eta_u \geq 2$, where k_{max} is the maximum resolved wavenumber, and η_u denotes the Kolmogorov length scale. The magnetic and cross helicities remain small in all simulation cases, to eliminate their impacts and emphasize the compressibility effect.

Simulation parameters are summarized in table 1. More simulation details can be found in tables I and II of the supplementary material available at https://doi.org/10.1017/jfm.2024.545. We note that the variations of M_t and δ_c within each series are small, implying their weak dependence on Reynolds number. It is also clear that the forcing parameter r_c has little impact on M_t for fixed Mach number, and $M_t/M \approx 2$ holds for all cases, whereas

Series	M	r_c	R_λ	M_t	$\delta_c = u_c'/u'$
A	0.1	0.10	50–252	0.20–0.21	0.36–0.41
B	0.1	0.50	32–230	0.20–0.21	0.61–0.65
C	0.1	0.90	23–268	0.20–0.24	0.76–0.85
D	0.3	0.10	50–386	0.61–0.64	0.33–0.34
E	0.3	0.50	36–376	0.64–0.68	0.55–0.63
F	0.3	0.75	30–250	0.66–0.69	0.70–0.74
P	0.2	0.85	40–357	0.42–0.45	0.80–0.82
Q	0.2	1.00	42–236	0.44–0.47	0.85–0.94

Table 1. Basic parameters and statistics of simulation series: M denotes the Mach number, r_c the forcing parameter, $R_\lambda = Re\,\langle\rho\rangle\, u'\lambda/\langle\mu\rangle$ the Taylor scale Reynolds number, $M_t = Mu'/\langle\sqrt{T/3}\rangle$ the turbulent Mach number, and $\delta_c = u_c'/u'$ the flow compressibility parameter.

the parameter δ_c obviously increases as r_c increases, and is almost independent of Mach number. Therefore, as in compressible HD turbulence (Donzis & John 2020), the nature of forcing has to be considered in addition to R_λ and M_t.

3. Results

By analysing selective DNS cases (see figure 1 in the supplementary material), it is found that the velocity field spectrum follows a classical incompressible $k^{-5/3}$ law for low to moderate δ_c, but shows k^{-2} behaviour for cases with high δ_c, due to the shock effects (Wang *et al.* 2013; Yang *et al.* 2016*a*). This different scaling behaviour suggests that the large-scale force can strongly influence the cascade process, and implies non-universality of compressible MHD turbulence associated with the dimensionless parameter $\delta_c = u_c'/u'$.

3.1. *The scaling of the relative dissipation rates*

The total dissipation consists of the viscous dissipation $\varepsilon_k = Re^{-1}\,\langle\sigma_{ij}S_{ij}/\rho\rangle$ and Ohmic dissipation $\varepsilon_m = Re_m^{-1}\,\langle\eta\boldsymbol{j}^2/\rho\rangle$. Moreover, the viscous dissipation ε_k can be decomposed as $\varepsilon_k = \varepsilon_s + \varepsilon_c + \varepsilon_n$. Here, the first term, $\varepsilon_s = Re^{-1}\,\langle\nu\boldsymbol{\omega}^2\rangle$, represents contributions by the solenoidal velocity field $\boldsymbol{u}_s$. The second component, $\varepsilon_c = (4/3)\,Re^{-1}\,\langle\nu\theta^2\rangle$, denotes the dilatational dissipation and is exclusively due to the dilatational motion $\boldsymbol{u}_c$. The mixed term $\varepsilon_n = 2\,Re^{-1}\,\langle\nu\boldsymbol{\nabla}\cdot(\boldsymbol{u}\cdot\boldsymbol{\nabla}\boldsymbol{u} - \theta\boldsymbol{u})\rangle$ vanishes if ν is uniform over the whole domain. The magnitude of $\varepsilon_n/\varepsilon_k$ remains small for all the simulation cases, hence the dissipation due to dilatational and shear motions can be viewed as decoupled.

The scaling of $\varepsilon_c/\varepsilon_s$ versus the parameter $\Lambda_c = E_c/E_s$ is shown in figure 1(*a*), where $E_s = \langle\rho\boldsymbol{u}_s^2/2\rangle$ and $E_c = \langle\rho\boldsymbol{u}_c^2/2\rangle$ denote the turbulent total energy of the solenoidal and compressive fields, respectively. One can see that all data points follow a simple scaling

$$\varepsilon_c/\varepsilon_s \approx E_c/E_s \approx \langle\boldsymbol{u}_c^2\rangle/\langle\boldsymbol{u}_s^2\rangle = \delta_c^2/(1-\delta_c^2), \tag{3.1}$$

especially for the cases with high Reynolds number $R_\lambda \geq 150$. This scaling was also observed in compressible HD turbulence (Donzis & John 2020).

Figure 1(*b*) shows the scaling of $\varepsilon_m/\varepsilon_k$, the ratio of Ohmic to viscous dissipation, as a function of $\Lambda_m = E_m/E_k$, where E_m and E_k denote the magnetic and kinetic energy, respectively. All simulations in our study are mechanically driven; hence the magnetic energy, maintained by the dynamo process, is much smaller than the kinetic energy ($\Lambda_m \lessapprox$

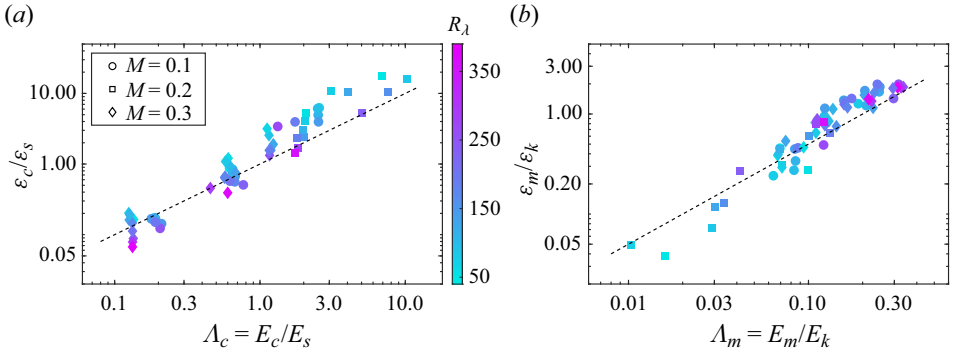

Figure 1. (*a*) The ratio of dilatational to solenoidal dissipation rate $\varepsilon_c/\varepsilon_s$ versus $\Lambda_c = E_c/E_s$, the ratio of solenoidal to dilatational energy. (*b*) The ratio of Ohmic to viscous dissipation $\varepsilon_m/\varepsilon_k$ versus $\Lambda_m = E_m/E_k$, the ratio of magnetic to kinetic energy. Here, only simulation cases with $R_\lambda \geq 50$ are taken into account, and the dashed lines indicate the linear scaling.

0.3 here). However, the magnetic dissipation can surpass the viscous dissipation when $\Lambda_m \gtrapprox 0.2$, suggesting that the magnetic field is dominated by the strong turbulent shear motions at small scales, such as current sheets. Moreover, all data points fit well with

$$\varepsilon_m/\varepsilon_k \approx g_m E_m/E_k, \tag{3.2}$$

with $g_m \approx 5.0$. This scaling remains robust over two orders of magnitude in $\varepsilon_m/\varepsilon_k$, implying that the characteristic time scales of magnetic and kinetic energy dissipation are of similar order. Figure 1(*b*) also shows that $\varepsilon_m/\varepsilon_k$ approximately increases as R_λ increases, implying that the nonlinear dynamo process is more efficient in maintaining small-scale magnetic field fluctuations at higher Reynolds number than at lower Reynolds number. Similar conclusions have been reached for IMHD turbulence (Linkmann *et al.* 2017).

3.2. *The normalized total dissipation rate*

As used in IMHD turbulence (Linkmann *et al.* 2015, 2017), the Elsässer variables $\boldsymbol{z}_\pm = \boldsymbol{u} \pm \boldsymbol{v}_A$ are introduced, where $\boldsymbol{v}_A = \boldsymbol{b}/\sqrt{\rho}$ denotes the magnetic fluctuations in Alfvén velocity unit. The r.m.s. values and integral length scales defined with respect to the Elsässer variables are $Z_\pm = \sqrt{(\langle \boldsymbol{z}_\pm^2 \rangle - \langle \boldsymbol{z}_\pm \rangle^2)/3}$ and $L_\pm = \pi/(2Z_\pm^2)\int_0^\infty k^{-1}\, E^\pm(k)\,\mathrm{d}k$, where $E^\pm(k)$ denotes the Elsässer energy spectrum such that $\int_0^\infty E^\pm(k)\,\mathrm{d}k = 3Z_\pm^2/2$. In analogy with the IMHD case (Linkmann *et al.* 2015, 2017), we define the dimensionless dissipation rate $\mathcal{C}_\varepsilon^\pm$ and the generalized large-scale Reynolds number $R_L^\pm$ as

$$\mathcal{C}_\varepsilon^\pm = \frac{\varepsilon L_\pm}{(Z_\pm)^2 Z_\mp}, \quad R_L^\pm = \frac{\langle \rho \rangle\, Z_\pm L_\mp}{\langle \mu \rangle}. \tag{3.3a,b}$$

In our simulations $Z_+ \approx Z_-$ and $L_+ \approx L_-$ since the cross-helicity $H_c = \langle \boldsymbol{u} \cdot \boldsymbol{b} \rangle$ remains negligible. Then $R_L^+ \approx R_L^-$ and $\mathcal{C}_\varepsilon^+ \approx \mathcal{C}_\varepsilon^-$ also hold (see figure 2 in the supplementary material). We focus on the relation between

$$\mathcal{C}_\varepsilon = \left(\mathcal{C}_\varepsilon^+ + \mathcal{C}_\varepsilon^-\right)/2 \tag{3.4}$$

and R_L^- to explore the dissipative anomaly in this paper.

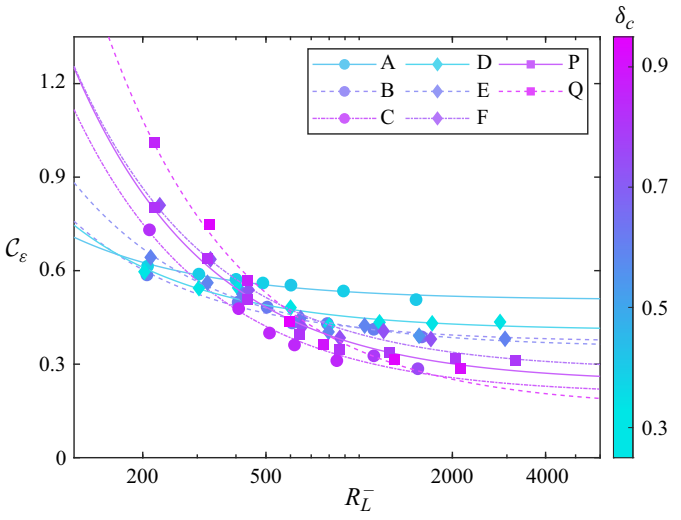

Figure 2. The normalized dissipation rate $\mathcal{C}_\varepsilon$ versus the generalized large-scale Reynolds number R_L^- for all simulation series, along with corresponding fitting curves (3.5). Here, the markers and lines are coloured by the values of compressibility parameter δ_c.

The model equation

$$\mathcal{C}_\varepsilon = \mathcal{C}_{\varepsilon,\infty} + \frac{\mathcal{D}}{R_L^-} + O\left[(R_L^-)^{-2}\right] \tag{3.5}$$

is often used to describe quantitatively the trend of dimensionless dissipation rate as Reynolds number increases (Linkmann *et al.* 2015, 2017; McComb *et al.* 2015; Bandyopadhyay *et al.* 2018), where $\mathcal{C}_{\varepsilon,\infty}$ is the asymptotic value of $\mathcal{C}_\varepsilon$ as R_L^- tends to infinity, and $\mathcal{D}$ is the coefficient of the first-order term. As suggested in Linkmann *et al.* (2015, 2017), the higher-order terms become important only for low Reynolds number cases, which is further discussed in the supplementary material.

The dimensionless dissipation rate $\mathcal{C}_\varepsilon$ as a function of generalized large-scale Reynolds number R_L^- is scattered in figure 2 for all simulation cases with $R_L^- \geq 150$, which fits well with the model (3.5). Here, the data points and fitting curves are coloured by the parameter δ_c to highlight the flow compressibility effect. The asymptotic dissipation rates $\mathcal{C}_{\varepsilon,\infty}$ remain positive, hence the dissipative anomaly holds generally in compressible MHD turbulence, even for flows with high compressibility.

3.3. *The compressibility effect on the dissipative anomaly*

As shown in figure 2, the compressibility depresses the normalized dissipation rate $\mathcal{C}_\varepsilon$ at high Reynolds number yet enhances it at low Reynolds number, indicating that $\mathcal{C}_{\varepsilon,\infty}$ decreases with increasing compressibility, but the coefficient $\mathcal{D}$ increases with the increase of flow compressibility. The estimated values of model coefficients $\mathcal{C}_{\varepsilon,\infty}$, $\mathcal{D}$ and the corresponding standard errors σ_C, σ_D are summarized in table 2. The values of $\overline{\delta_c}$, denoting the mean value of δ_c within each DNS series, are also reported to clearly show the level of compressibility of each simulation series. Moreover, the results of incompressible isotropic driven HD turbulence (McComb *et al.* 2015) and MHD turbulence (Bandyopadhyay *et al.* 2018) are included for comparison. (Here, the result from Bandyopadhyay *et al.* (2018)

Series	$\overline{\delta_c}$	$\mathcal{C}_{\varepsilon,\infty}$	σ_C	$\mathcal{D}$	σ_D
A	0.39	0.506	0.007	24.2	2.6
B	0.62	0.370	0.010	46.6	4.2
C	0.82	0.198	0.016	110.6	6.9
D	0.33	0.410	0.012	40.3	5.0
E	0.59	0.351	0.012	64.1	5.1
F	0.73	0.280	0.021	117.1	9.1
P	0.81	0.241	0.016	121.2	7.3
Q	0.89	0.159	0.022	184.7	9.2
HD	0.00	0.468	0.006	18.9	1.3
IMHD	0.00	0.520	0.014	18.0	1.0

Table 2. Summary of estimated values for the asymptotic dimensionless dissipation rate $\mathcal{C}_{\varepsilon,\infty}$ and model coefficient $\mathcal{D}$ from different simulation series and references. Here, σ_C, σ_D refer to the standard errors of $\mathcal{C}_{\varepsilon,\infty}, \mathcal{D}$ in the fitting procedure, respectively, and $\overline{\delta_c}$ denotes the mean value of δ_c within each simulation series. The results of HD turbulence (McComb *et al.* 2015) and MHD turbulence (Bandyopadhyay *et al.* 2018) are included for comparison.

is multiplied by factor 2 due to the different definitions of $\mathcal{C}_\varepsilon$.) One can see that the values of $\mathcal{C}_{\varepsilon,\infty}$ and $\mathcal{D}$ of series A (with weak compressibility) are quite close to those in incompressible cases. Also, the standard errors are significantly small compared to the estimated values, for all simulation series, indicating the credibility of the fitting model (3.5). Based on the von Kármán–Howarth (vKH) equation (de Kármán & Howarth 1938; Chandrasekhar 1951; Politano & Pouquet 1998) that describes the evolution of correlation functions in turbulence, the asymptotic value $\mathcal{C}_{\varepsilon,\infty}$ represents the flux of total energy across scales in a well scale-separated inertial range (Linkmann *et al.* 2015, 2017; McComb *et al.* 2015). Our results show that the flow compressibility can strongly depress the energy flux, and again indicate the non-universality of energy transfer and dissipation processes in compressible MHD turbulence.

To quantify the compressibility effect on the dissipative anomaly in compressible MHD (CMHD) turbulence, the asymptotic dimensionless dissipation rate $\mathcal{C}_{\varepsilon,\infty}$ and model coefficient $\mathcal{D}$ from all simulation series are scattered. Figure 3(*a*) shows the trend of $\mathcal{C}_{\varepsilon,\infty}$ versus $\overline{\delta_c}^2 \approx \overline{E_c/E_k}$, along with the incompressible values. Surprisingly, a simple scaling

$$\mathcal{C}_{\varepsilon,\infty} = \mathcal{C}_0 - \mathcal{C}_1 \overline{\delta_c}^2 \tag{3.6}$$

is observed, where $\mathcal{C}_0 = 0.517 \pm 0.021$ is quite close to the asymptotic value in the IMHD case, and $\mathcal{C}_1 = 0.436 \pm 0.042$ denotes the fitting coefficient. Also, the positivity of the limiting value $\mathcal{C}_{\varepsilon,\infty}(\overline{\delta_c} \to 1) = \mathcal{C}_0 - \mathcal{C}_1 = 0.081 \pm 0.027$ suggests that the dissipative anomaly still holds even in the MHD turbulence with extremely high compressibility. Figure 3(*b*) depicts the scaling of $\mathcal{D}/\mathcal{D}_0$, the normalized model coefficient as flow compressibility increases, where $\mathcal{D}_0 = 18.0$ denotes the model coefficient in the IMHD case. The plot indicates that the scaling

$$\mathcal{D}/\mathcal{D}_0 = 1 + \mathcal{D}_1 \overline{\delta_c}^4 \tag{3.7}$$

holds approximately, with fitting parameter $\mathcal{D}_1 = 13.5$.

Based on the above simple scaling of $\mathcal{C}_{\varepsilon,\infty}, \mathcal{D}$ versus δ_c, the model equation (3.5) that expresses the dimensionless dissipation rate $\mathcal{C}_\varepsilon$ in terms of the generalized Reynolds

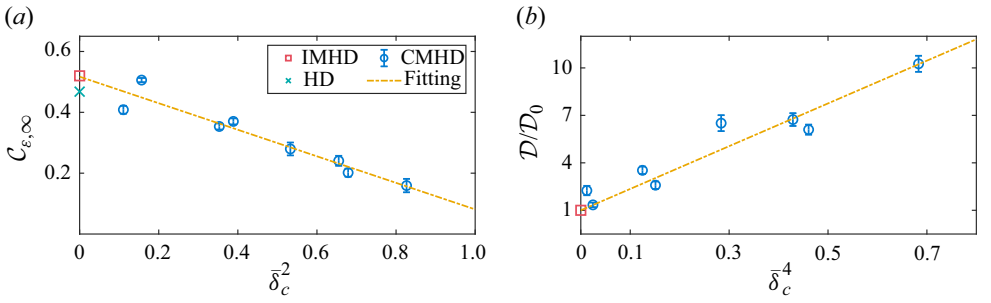

Figure 3. The trend of the asymptotic normalized dissipation rate $\mathcal{C}_{\varepsilon,\infty}$ and model coefficient $\mathcal{D}$ as flow compressibility changes: (*a*) $\mathcal{C}_{\varepsilon,\infty}$ versus $\overline{\delta_c}^2$; (*b*) $\mathcal{D}/\mathcal{D}_0$ versus $\overline{\delta_c}^4$. The dashed lines indicate the linear regression, and the error bars represent the standard errors in fitting procedure.

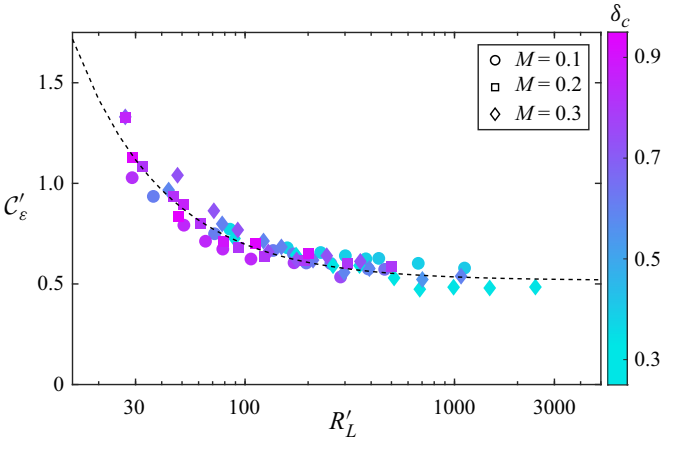

Figure 4. Modified normalized dissipation rate $\mathcal{C}'_\varepsilon$ versus modified Reynolds number R'_L for all simulations. The dashed line corresponds to (3.8), the same form as in the IMHD case.

number R_L^- can be transformed into a unified form,

$$\mathcal{C}'_\varepsilon = \mathcal{C}_0 + \frac{\mathcal{D}_0}{R'_L}, \tag{3.8}$$

similar in form to the model for the IMHD case. In particular, the modified dimensionless dissipation rate $\mathcal{C}'_\varepsilon$ and the modified large-scale Reynolds number R'_L are defined as

$$\mathcal{C}'_\varepsilon = \mathcal{C}_\varepsilon + \mathcal{C}_1\delta_c^2, \quad R'_L = \frac{R_L^-}{1 + \mathcal{D}_1\delta_c^4}, \tag{3.9a,b}$$

in which the correction from compressibility is implemented. To emphasize the efficacy of this re-scaling, the values of $\mathcal{C}'_\varepsilon$ and R'_L for all DNS cases are scattered in figure 4. Notably, all data points, regardless of their level of flow compressibility, collapse along the model equation (3.8).

However, it is essential to highlight that the aforementioned results cannot be considered as universal. In particular, the unified model equation was obtained under the specific conditions of isotropy and zero helicities, and fixed fluid parameters, including $Pr = 0.704$

and $T_0 = 273.15$ K. While these conditions and parameters may not alter the qualitative form of the basic model equation (3.5), the model coefficients $\mathcal{C}_{\varepsilon,\infty}$, $\mathcal{D}$ will likely depend on various flow parameters and may not follow simple scaling laws similar to (3.6)–(3.7). For instance, prior studies have showed notable dependencies of the asymptotic dissipation rate $\mathcal{C}_{\varepsilon,\infty}$ on cross-helicity, magnetic helicity (Linkmann *et al.* 2015, 2017) and mean magnetic field (Bandyopadhyay *et al.* 2018) in IMHD turbulence. Therefore, in this study, the unified (3.8) serves as an alternative representation to illustrate the scaling relations between model coefficients and compressibility parameters, and does not imply the universality of dissipation in compressible MHD turbulence. We expect that exploring compressible MHD turbulence under more general configurations may yield further intriguing findings.

4. Conclusions

In conclusion, by direct numerical simulation, we explored the non-universality in compressible MHD turbulence, emphasizing the effect of compressibility (which is mainly controlled by the forcing scheme) on the dissipative anomaly, a feature of substantial importance in turbulence theory and modelling. By studying the scaling between the ratio of dissipation rates and the ratio of energy, it is found that the characteristic time scales of viscous dissipation and magnetic dissipation are of the same order of magnitude, and a similar result was verified for the kinetic dissipation process induced by dilatation and shearing processes.

In the compressible MHD turbulence, the dimensionless total dissipation rate $\mathcal{C}_\varepsilon$ approaches asymptotically a non-zero value $\mathcal{C}_{\varepsilon,\infty}$ for increasing generalized large-scale Reynolds number R_L^-. That is, as in HD and IMHD turbulence, the dissipative anomaly is present in compressible MHD turbulence as well. Moreover, the relation between $\mathcal{C}_\varepsilon$ and R_L^- can be described by the simple model equation (3.5). The values of $\mathcal{C}_{\varepsilon,\infty}$ and model coefficient $\mathcal{D}$ of simulation series show obvious differences, suggesting the non-universality of compressible MHD turbulence induced by different levels of flow compressibility. Specifically, a decreasing trend was found for $\mathcal{C}_{\varepsilon,\infty}$ with the increase of δ_c, implying that the compressibility can strongly depress the energy flux in compressible MHD turbulence. It was also found that the model coefficient $\mathcal{D}$ would increase dramatically for enhanced flow compressibility. Further numerical results find that $\mathcal{C}_{\varepsilon,\infty}$ and $\mathcal{D}$ exhibit simple scaling with respect to the compressibility parameter δ_c. Based on this finding, we introduced a modified normalized dissipation rate $\mathcal{C}'_\varepsilon$ and a modified large-scale Reynolds number R'_L, which incorporate the compressibility effect. In terms of these, we find the quantitative relation (3.5) transformed into one unified equation (3.8), in which the asymptotic value and model coefficient correspond to the IMHD case. These results inform understanding of the relationship between incompressible and compressible MHD flow models, and provide a quantitative assessment of the influence of compressibility on energy transfer. Our findings hold potential relevance to various studies focusing on real physics systems, particularly in plasma turbulence domains like the solar wind. For instance, our numerical results could provide valuable guidance to simplify the complex formulations of exact laws in compressible MHD turbulence (Banerjee & Galtier 2013; Andrés & Sahraoui 2017). Moreover, these exact relations are frequently utilized to estimate energy dissipation and particle heating in spacecraft observations (Sorriso-Valvo *et al.* 2007; Wan *et al.* 2012, 2016; Andrés *et al.* 2018; Hadid *et al.* 2018; Simon & Sahraoui 2021; Yang *et al.* 2022; Jiang *et al.* 2023; Marino & Sorriso-Valvo 2023). This is especially pertinent in collisionless plasmas where classical definitions of viscosity and

resistivity are inapplicable, making direct dissipation rate calculations from observational data unfeasible.

Supplementary material. Supplementary material is available at https://doi.org/10.1017/jfm.2024.545.

Funding. This work was supported by NSFC (grant nos 12225204 and 11902138), Department of Science and Technology of Guangdong Province (grant nos 2019B21203001 and 2020B1212030001), and the Shenzhen Science and Technology Program (grant no. KQTD20180411143441009). Y.Y. and W.H.M. were partially supported by US NSF grant AGS-2108834. Numerical simulations were supported by the Center for Computational Science and Engineering of Southern University of Science and Technology.

Declaration of interests. The authors report no conflict of interest.

Author ORCIDs.
William H. Matthaeus https://orcid.org/0000-0001-7224-6024;
Bin Jiang https://orcid.org/0000-0002-4858-0505;
Minping Wan https://orcid.org/0000-0001-5891-9579.

References

ALUIE, H. 2017 Coarse-grained incompressible magnetohydrodynamics: analyzing the turbulent cascades. *New J. Phys.* **19** (2), 025008.

ANDRÉS, N. & SAHRAOUI, F. 2017 Alternative derivation of exact law for compressible and isothermal magnetohydrodynamics turbulence. *Phys. Rev.* E **96** (5), 053205.

ANDRÉS, N., SAHRAOUI, F., GALTIER, S., HADID, L.Z., DMITRUK, P. & MININNI, P. 2018 Energy cascade rate in isothermal compressible magnetohydrodynamic turbulence. *J. Plasma Phys.* **84** (4), 905840404.

BANDYOPADHYAY, R., OUGHTON, S., WAN, M., MATTHAEUS, W.H., CHHIBER, R. & PARASHAR, T.N. 2018 Finite dissipation in anisotropic magnetohydrodynamic turbulence. *Phys. Rev.* X **8** (4), 041052.

BANERJEE, S. & GALTIER, S. 2013 Exact relation with two-point correlation functions and phenomenological approach for compressible magnetohydrodynamic turbulence. *Phys. Rev.* E **87** (1), 013019.

CHANDRASEKHAR, S. 1951 The invariant theory of isotropic turbulence in magneto-hydrodynamics. *Proc. R. Soc. Lond.* A **204** (1079), 435–449.

CONSTANTIN, P., WEINAN, E. & TITI, E.S. 1994 Onsager's conjecture on the energy conservation for solutions of Euler's equation. *Commun. Math. Phys.* **165** (1), 207–209.

DALLAS, V. & ALEXAKIS, A. 2014 The signature of initial conditions on magnetohydrodynamic turbulence. *Astrophys. J.* **788** (2), L36.

DONZIS, D.A. & JOHN, J.P. 2020 Universality and scaling in homogeneous compressible turbulence. *Phys. Rev. Fluids* **5** (8), 084609.

DUCHON, J. & ROBERT, R. 2000 Inertial energy dissipation for weak solutions of incompressible Euler and Navier–Stokes equations. *Nonlinearity* **13** (1), 249–255.

EYINK, G.L. 1994 Energy dissipation without viscosity in ideal hydrodynamics. I. Fourier analysis and local energy transfer. *Physica* D **78** (3–4), 222–240.

EYINK, G.L. & DRIVAS, T.D. 2018 Cascades and dissipative anomalies in compressible fluid turbulence. *Phys. Rev.* X **8** (1), 011022.

FRISCH, U. 1995 *Turbulence: The Legacy of A.N. Kolmogorov*. Cambridge University Press.

GALTIER, S. 2018 On the origin of the energy dissipation anomaly in (Hall) magnetohydrodynamics. *J. Phys.* A **51** (20), 205501.

GOTO, S. & VASSILICOS, J.C. 2009 The dissipation rate coefficient of turbulence is not universal and depends on the internal stagnation point structure. *Phys. Fluids* **21** (3), 035104.

HADID, L.Z., SAHRAOUI, F., GALTIER, S. & HUANG, S.Y. 2018 Compressible magnetohydrodynamic turbulence in the Earth's magnetosheath: estimation of the energy cascade rate using *in situ* spacecraft data. *Phys. Rev. Lett.* **120** (5), 055102.

JIANG, B., LI, C., YANG, Y., ZHOU, K., MATTHAEUS, W.H. & WAN, M. 2023 Energy transfer and third-order law in forced anisotropic magneto-hydrodynamic turbulence with hyper-viscosity. *J. Fluid Mech.* **974**, A20.

JOHN, J.P., DONZIS, D.A. & SREENIVASAN, K.R. 2021 Does dissipative anomaly hold for compressible turbulence? *J. Fluid Mech.* **920**, A20.

KANEDA, Y., ISHIHARA, T., YOKOKAWA, M., ITAKURA, K. & UNO, A. 2003 Energy dissipation rate and energy spectrum in high resolution direct numerical simulations of turbulence in a periodic box. *Phys. Fluids* **15** (2), L21–L24.

DE KÁRMÁN, T. & HOWARTH, L. 1938 On the statistical theory of isotropic turbulence. *Proc. R. Soc. Lond.* A **164** (917), 192–215.

KOLMOGOROV, A.N. 1941*a* Dissipation of energy in the locally isotropic turbulence. *Dokl. Akad. Nauk SSSR*. **32**, 19–21.

KOLMOGOROV, A.N. 1941*b* The local structure of turbulence in incompressible viscous fluid for very large Reynolds numbers. In *Dokl. Akad. Nauk SSSR*, vol. 30, pp. 299–303.

KOLMOGOROV, A.N. 1941*c* On degeneration (decay) of isotropic turbulence in an incompressible viscous liquid. In *Dokl. Akad. Nauk SSSR*, vol. 31, pp. 538–540.

LINKMANN, M.F., BERERA, A. & GOLDSTRAW, E.E. 2017 Reynolds-number dependence of the dimensionless dissipation rate in homogeneous magnetohydrodynamic turbulence. *Phys. Rev.* E **95** (1), 013102.

LINKMANN, M.F., BERERA, A., MCCOMB, W.D. & MCKAY, M.E. 2015 Nonuniversality and finite dissipation in decaying magnetohydrodynamic turbulence. *Phys. Rev. Lett.* **114** (23), 235001.

MARINO, R., FERACO, F., PRIMAVERA, L., PUMIR, A., POUQUET, A., ROSENBERG, D. & MININNI, P.D. 2022 Turbulence generation by large-scale extreme vertical drafts and the modulation of local energy dissipation in stably stratified geophysical flows. *Phys. Rev. Fluids* **7** (3), 033801.

MARINO, R. & SORRISO-VALVO, L. 2023 Scaling laws for the energy transfer in space plasma turbulence. *Phys. Rep.* **1006**, 1–144.

MAZELLIER, N. & VASSILICOS, J.C. 2008 The turbulence dissipation constant is not universal because of its universal dependence on large-scale flow topology. *Phys. Fluids* **20** (1), 015101.

MCCOMB, W.D., BERERA, A., YOFFE, S.R. & LINKMANN, M.F. 2015 Energy transfer and dissipation in forced isotropic turbulence. *Phys. Rev.* E **91** (4), 043013.

MININNI, P.D. & POUQUET, A. 2009 Finite dissipation and intermittency in magnetohydrodynamics. *Phys. Rev.* E **80** (2), 025401.

ONSAGER, L. 1949 Statistical hydrodynamics. *Il Nuovo Cimento* **6** (S2), 279–287.

PEARSON, B. & FOX-KEMPER, B. 2018 Log-normal turbulence dissipation in global ocean models. *Phys. Rev. Lett.* **120**, 094501.

PEARSON, B.R., YOUSEF, T.A., HAUGEN, N.E.L., BRANDENBURG, A. & KROGSTAD, P.-Å. 2004 Delayed correlation between turbulent energy injection and dissipation. *Phys. Rev.* E **70** (5), 056301.

POLITANO, H. & POUQUET, A. 1998 Von Kármán–Howarth equation for magnetohydrodynamics and its consequences on third-order longitudinal structure and correlation functions. *Phys. Rev.* E **57** (1), R21–R24.

POUQUET, A., ROSENBERG, D. & MARINO, R. 2019 Linking dissipation, anisotropy, and intermittency in rotating stratified turbulence at the threshold of linear shear instabilities. *Phys. Fluids* **31** (10), 105116.

SIMON, P. & SAHRAOUI, F. 2021 General exact law of compressible isentropic magnetohydrodynamic flows: theory and spacecraft observations in the solar wind. *Astrophys. J.* **916** (1), 49.

SORRISO-VALVO, L., MARINO, R., CARBONE, V., NOULLEZ, A., LEPRETI, F., VELTRI, P., BRUNO, R., BAVASSANO, B. & PIETROPAOLO, E. 2007 Observation of inertial energy cascade in interplanetary space plasma. *Phys. Rev. Lett.* **99** (11), 115001.

SREENIVASAN, K.R. 1984 On the scaling of the turbulence energy dissipation rate. *Phys. Fluids* **27** (5), 1048.

SREENIVASAN, K.R. 1998 An update on the energy dissipation rate in isotropic turbulence. *Phys. Fluids* **10** (2), 528–529.

TAYLOR, G.I. 1935 Statistical theory of turbulence. *Proc. R. Soc. Lond.* A **151** (873), 421–444.

VASSILICOS, J.C. 2015 Dissipation in turbulent flows. *Annu. Rev. Fluid Mech.* **47** (1), 95–114.

WAN, M., MATTHAEUS, W.H., KARIMABADI, H., ROYTERSHTEYN, V., SHAY, M., WU, P., DAUGHTON, W., LORING, B. & CHAPMAN, S.C. 2012 Intermittent dissipation at kinetic scales in collisionless plasma turbulence. *Phys. Rev. Lett.* **109** (19), 195001.

WAN, M., MATTHAEUS, W.H., ROYTERSHTEYN, V., PARASHAR, T.N., WU, P. & KARIMABADI, H. 2016 Intermittency, coherent structures and dissipation in plasma turbulence. *Phys. Plasmas* **23** (4), 042307.

WANG, J., SHI, Y., WANG, L.-P., XIAO, Z., HE, X.T. & CHEN, S. 2012 Effect of compressibility on the small-scale structures in isotropic turbulence. *J. Fluid Mech.* **713**, 588–631.

WANG, J., WANG, L.-P., XIAO, Z., SHI, Y. & CHEN, S. 2010 A hybrid numerical simulation of isotropic compressible turbulence. *J. Comput. Phys.* **229** (13), 5257–5279.

WANG, J., YANG, Y., SHI, Y., XIAO, Z., HE, X.T. & CHEN, S. 2013 Cascade of kinetic energy in three-dimensional compressible turbulence. *Phys. Rev. Lett.* **110**, 214505.

YANG, Y., MATTHAEUS, W.H., ROY, S., ROYTERSHTEYN, V., PARASHAR, T.N., BANDYOPADHYAY, R. & WAN, M. 2022 Pressure–strain interaction as the energy dissipation estimate in collisionless plasma. *Astrophys. J.* **929** (2), l42.

YANG, Y., MATTHAEUS, W.H., SHI, Y., WAN, M. & CHEN, S. 2017 Compressibility effect on coherent structures, energy transfer, and scaling in magnetohydrodynamic turbulence. *Phys. Fluids* **29** (3), 035105.

YANG, Y., SHI, Y., WAN, M., MATTHAEUS, W.H. & CHEN, S. 2016*a* Energy cascade and its locality in compressible magnetohydrodynamic turbulence. *Phys. Rev.* E **93** (6), 061102.

YANG, Y., WAN, M., MATTHAEUS, W.H. & CHEN, S. 2021 Energy budget in decaying compressible MHD turbulence. *J. Fluid Mech.* **916**, A4.

YANG, Y., WAN, M., SHI, Y., YANG, K. & CHEN, S. 2016*b* A hybrid scheme for compressible magnetohydrodynamic turbulence. *J. Comput. Phys.* **306**, 73–91.